

# Influence of Copolymer Composition on Non-Fickian Water Transport through Glassy Copolymers

NANCY M. FRANSON \* and NIKOLAOS A. PEPPAS, *School of Chemical Engineering, Purdue University, West Lafayette, Indiana 47907*

## Synopsis

The dynamic swelling behavior of poly(2-hydroxyethyl methacrylate-co-methyl methacrylate) and poly(2-hydroxyethyl methacrylate-co-*N*-vinyl-2-pyrrolidone) in water was followed at 37°C. The results were analyzed in terms of a simple non-Fickian transport equation, which expresses the fractional penetrant uptake as an exponential function of the diffusion time. The exponent  $n$ , which indicates Fickian or non-Fickian transport mechanism, was correlated to the content of the more hydrophilic component of the copolymer. Photomicrographs obtained with polarized light offer new information about the position and movement of the penetrant front in glassy, hydrophilic polymers.

## INTRODUCTION

Isothermal penetrant transport through glassy polymers is usually accompanied by transitions from the glassy to the rubbery state which control the mechanism of penetrant diffusion. During this process, a sharp penetration front is observed which separates the outer rubbery (gel-like) region from the inner glassy core. Macromolecular relaxations in the proximity of this penetration front influence the mechanism of penetrant transport.<sup>1</sup>

Alfrey et al.<sup>2</sup> set the characteristics of non-Fickian transport behavior and coined the term "Case-II transport" for the special case where the penetrant front moves with constant velocity  $v$ . Peterlin<sup>3,4</sup> offered a non-Fickian equation incorporating the velocity  $v$  into the Fickian equation, which can be used to describe certain types of anomalous diffusion. He provided mathematical solutions for a variety of boundary conditions and geometries. Wang et al.<sup>5</sup> provided further mathematical analysis of this problem and offered experimental evidence that Case-II transport could be observed with certain solvents in poly(vinyl chloride)<sup>6</sup> and poly(methyl methacrylate).<sup>7</sup>

Relaxation-controlled transport mechanisms may be predicted by calculating the diffusional Deborah number,  $De$ , which is defined as the ratio of the characteristic relaxation time of the polymer to the characteristic diffusion time of the penetrant. Vrentas et al.<sup>8,9</sup> observed that when  $De \approx 1$  relaxation controls the diffusion process and non-Fickian mechanisms predominate, whereas for values of  $De \gg 1$  or  $De \ll 1$  the mechanisms are Fickian. More recent work by Astarita and Sarti<sup>10,11</sup> and Thomas and Windle<sup>12,13</sup> has addressed novel aspects of modeling of relaxation-controlled penetrant transport.

Experimental evidence and theoretical analysis of anomalous penetrant

\* Present address: Department of Applied Mechanics and Engineering Sciences, University of California at San Diego, LaJolla, CA 92093.

transport indicate that parameters which affect macromolecular relaxations influence the transport mechanism as well. These include molecular weight, molecular weight distribution, and degree of crosslinking of the polymer, physicochemical properties of the penetrant, and penetrant activity. Of particular interest to our group are phenomena related to penetrant transport in cross-linked, glassy polymers, especially copolymers containing a hydrophilic moiety.

Although numerous studies of diffusion of organic vapors or organic liquids have been published, studies on water transport in hydrophilic glassy copolymers are scarce, probably because of associated problems due to hydrogen bonding often observed with these systems. Recently, Hopfenberg et al.<sup>14,15</sup> studied the dynamic water swelling of various grades of poly(ethylene-co-vinyl alcohol) containing 0.7–0.97 mole fraction vinyl alcohol and observed Case-II or super-Case-II transport, depending on the content of vinyl alcohol in the copolymers.

Here we present studies on the non-Fickian transport of water in the initially glassy copolymers poly(2-hydroxyethyl methacrylate-co-*N*-vinyl-2-pyrrolidone) [P(HEMA-co-NVP)] and poly(2-hydroxyethyl methacrylate-co-methyl methacrylate) [P(HEMA-co-MMA)] with HEMA content varying over a wide range of mole fractions.

## EXPERIMENTAL

### Materials

HEMA (Aldrich Chemical Co., Milwaukee, Wisc.) and MMA (Eastman Kodak Co., Rochester, N.Y.) monomers were vacuum distilled at 67°C/3.5 mm Hg and 30°C/15 mm Hg, respectively. Bulk copolymerizations of 0.5–0.9 mole fraction HEMA and 0.5–0.1 mole fraction MMA were initiated with 0.5 wt % benzoyl peroxide. The polymerizations were carried out in polyethylene vials at  $60 \pm 1^\circ\text{C}$  for 12 h.

NVP monomer (Aldrich Chemical Co., Milwaukee, Wisc.) was vacuum distilled at 66°C/1.5 mm Hg. Mixtures of 0.40–0.90 mole fraction HEMA and 0.60–0.10 mole fraction NVP were initiated with 0.2 wt % azobisisobutyronitrile (AIBN). Some of the samples were crosslinked with 0.8 wt % ethylene glycol dimethacrylate (EGDMA). The reaction mixtures were flushed with nitrogen to rid the system of oxygen and sealed in polyethylene vials. The bulk copolymerizations were carried out at  $40 \pm 1^\circ\text{C}$  for the first 3 h of the 48-h reaction period, followed by a gradual rise of the temperature to  $80 \pm 1^\circ\text{C}$ . This procedure was employed (i) to prevent bubble formation in the copolymers which was observed when polymerization was carried out at 60°C and (ii) to allow the reaction to go to completion.

Pure PHEMA was also prepared by these techniques. The homopolymers and copolymers were obtained in transparent cylinders of 1.5 cm diameter and 3 cm height, which were cut with a lathe into 1 mm disks.

### Methods

In preparation for the swelling studies, all samples were dried in a vacuum oven at 50°C for 3 days to remove internal stresses and residual water that may have been absorbed from the atmosphere. The samples were weighed and the volumes

determined by the buoyancy method by weighing them in air and in heptane.

The samples were swollen in deionized water at  $37 \pm 0.5^\circ\text{C}$ . Dynamic swelling curves were obtained by periodically removing the samples from the water, blotting excess water from the surface, and weighing. When equilibrium was attained, the volumes in the swollen state were measured as described previously. The samples were dried to constant weight and the swelling procedure repeated.

The motion of the penetrant front was followed by taking photomicrographs of cylindrical samples during swelling. The penetrant front was visualized by placing a polarizing filter below the sample with a second polarizing filter on the camera situated  $90^\circ$  from the first. The cross-polarized light resulting from this filter arrangement and a light source beneath the sample allowed the stresses resulting from the glassy to rubbery transition to be recorded.

## RESULTS AND DISCUSSION

Both copolymer systems studied were crosslinked by chain transfer (in the absence of external crosslinking agent) or by added EGDMA. Radical bulk polymerizations of methacrylates are known to produce polymers which swell in good solvents without dissolving. Therefore, even in systems of HEMA and MMA reacted in the absence of external crosslinking agent, EGDMA, crosslinking can occur by radical chain transfer mechanisms.<sup>16</sup> In addition, HEMA monomer contains diester (EGDMA) as an impurity which cannot be removed by distillation.<sup>17</sup>

### Penetration Front

The dynamic swelling studies of these copolymers in water offer important new qualitative and quantitative information on the Fickian and anomalous transport of liquids through hydrophilic, glassy polymers. Qualitative information is provided by photomicrographs showing the motion of the penetrant front as swelling progresses.

Figure 1 shows the penetrant front position for a P(HEMA-co-MMA) disc with 0.90 mole fraction HEMA. It is evident that there is a sharp front which is a necessary criterion for Case-II transport. The position of the expanding outer polymer front is designated by A while the position of the penetrant front separating the rubbery from the glassy state is designated by B. A distinct zone C of significantly different refractive index is observed behind the penetrant front B. This is a region where macromolecular relaxations are still prominent. The thickness of zone C depends on time and the hydrophilicity of the copolymer. The region between the front A and region C is a swollen, rubbery copolymer, effectively at mechanical equilibrium. Stress lines can be observed within region C, but no further quantitative analysis can be achieved with this simple photographic technique. Moiré patterns analysis may be more appropriate for the investigation of these systems.<sup>18</sup>

To examine the effect of time on the thickness  $\delta$  of region C and to analyze the time-dependence of the polymer front A and the penetrant front B, several studies were conducted with glassy PHEMA homopolymers. These results are presented in Table I. The thickness  $\delta$  increases with increasing diffusion time, probably demonstrating increased relaxation of the macromolecular chains. In

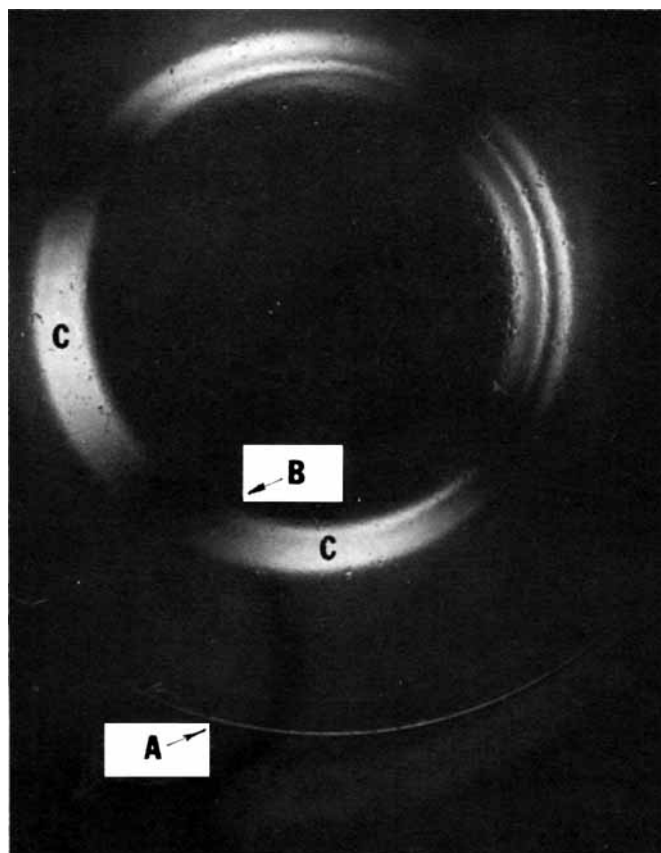


Fig. 1. Photomicrograph of a dynamically swelling P(HEMA-co-MMA) disk with 0.90 mole fraction HEMA: (A) polymer front; (B) penetrant front; (C) region of macromolecular relaxations.

addition, the positions of the fronts  $X_1$  and  $X_2$  cannot be fitted either to linear or to  $t^{1/2}$  functions of diffusion time, suggesting that water transport in these

TABLE I  
Polymer and Penetrant Front Position<sup>a</sup> during Dynamic Water Swelling of PHEMA Homopolymers at 37°C

Sample	Diffusion time (h)	Polymer front position $X_1$ (mm)	Penetrant front position $X_2$ (mm)	Thickness of region C, $\delta$ (mm)
Pure crosslinked PHEMA	0	(6.84)	(6.84)	0
	20	7.35	4.87	0.13
	28	7.54	4.07	0.37
	34	7.48	3.81	0.47
	44	7.61	3.67	0.53
	52	7.61	3.01	0.53
EGDMA-crosslinked PHEMA	0	6.84	6.84	0
	20	7.53	4.07	0.23
	28	7.54	3.70	0.33
	34	7.61	3.54	0.73
	52	7.61	2.62	—

<sup>a</sup> Position determined from the center of the disks.  $X_1$  is the position of front A and  $X_2$  is the position of front B (see Fig. 1).

two homopolymers is non-Fickian. Typical velocities of the penetration front B in the same period of 20–28 h were calculated as  $2.8 \times 10^{-6}$  cm/s for the crosslinked PHEMA samples and  $1.3 \times 10^{-6}$  cm/s for the EGDMA-crosslinked samples. Both values agree by order of magnitude with the velocities reported by Astarita and Joshi<sup>19</sup> for saline and ethanol transport in PHEMA.

A somewhat different penetrant front behavior was observed with water transport in P(HEMA-co-NVP) samples. Figures 2 and 3 show photomicrographs of a disc of P(HEMA-co-NVP) with 0.60 mole fraction NVP at the times 4 and 8 h, respectively. Here a single penetrant front is observed, and region C is diminished. Figure 3 shows a region D, where the rubbery position of the polymer had crazed due to excessive stresses in the system.

### Equilibrium Swelling

Data from the swelling studies are expressed in terms of water uptake  $q$ , defined as the weight of water imbibed by the sample per unit weight of dry polymer. In all cases the data are normalized with respect to the weight of the sample before swelling regardless of the past swelling history of the sample.

Values of the maximum water uptake  $q_m$  for the various compositions of the two copolymers studied are given in Table II. The values of  $q_m$  for P(HEMA-co-MMA) increase as the amount of HEMA, the more hydrophilic component,

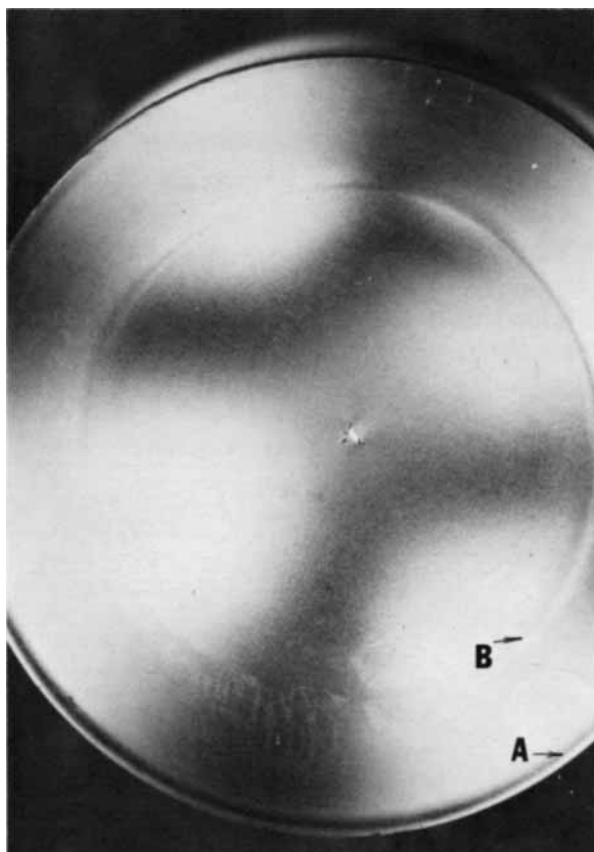


Fig. 2. Photomicrograph of a dynamically swelling P(HEMA-co-NVP) disk with 0.60 mole fraction NVP after 4 h: (A) polymer front; (B) penetrant front.

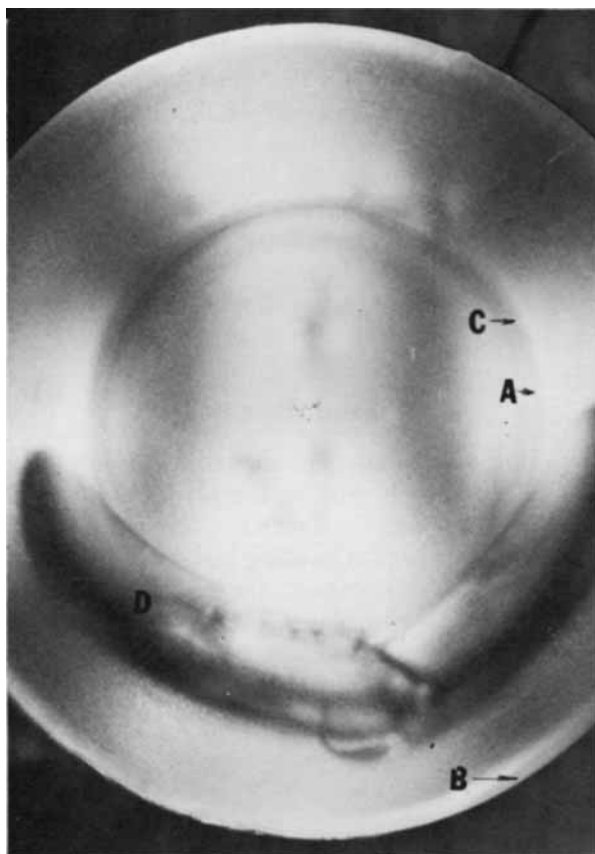


Fig. 3. Photomicrograph of a dynamically swelling P(HEMA-co-NVP) disk with 0.60 mole fraction NVP after 8 h: (A) penetrant front; (B) polymer front; (C) region of macromolecular relaxations; (D) region of crazing of the rubbery portion.

in the copolymer is increased. EGDMA-crosslinked samples swell slightly less than samples prepared without the addition of EGDMA. This trend indicates

TABLE II  
Equilibrium Water Uptake of Copolymers

Mole fraction HEMA	Mole fraction MMA	Mole fraction NVP	Wt % EGDMA	$q_m \pm sd$	Number of samples
0.5	0.5	—	—	$0.1554 \pm 0.0077$	6
0.7	0.3	—	—	$0.2504 \pm 0.0053$	7
0.8	0.2	—	—	$0.3203 \pm 0.0083$	7
0.9	0.1	—	—	$0.4141 \pm 0.0179$	6
1.0	—	—	—	$0.5927 \pm 0.0185$	6
1.0	—	—	0.8	$0.5461 \pm 0.0086$	2
1.0	—	—	—	$0.5927 \pm 0.0185$	6
0.9	—	0.1	—	$0.4643 \pm 0.0150$	2
0.8	—	0.2	—	$0.4824 \pm 0.0023$	2
0.7	—	0.3	—	$0.5668 \pm 0.0058$	3
1.0	—	—	0.8	$0.5461 \pm 0.0086$	2
0.8	—	0.2	0.8	0.4740	1
0.6	—	0.4	0.8	0.6802	1
0.4	—	0.6	0.8	1.3603	1

that as the hydrophilicity of the system increases, the maximum water uptake increases.

The value of  $q_m$  for P(HEMA-co-NVP) samples prepared without added crosslinking agent increases within the series as the more hydrophilic component, NVP, increases. However, all values for the copolymer are lower than those for pure PHEMA. When crosslinking agent is added to the system, the trend within the series is still present; only the material containing 0.2 mole fraction NVP swells less than pure, EGDMA-crosslinked PHEMA.

These results may be explained by unreacted NVP monomer in the system due to its low reactivity ratio ( $r_1 = 4.37$  HEMA,  $r_2 = 0.038$  NVP,  $r_1 r_2 = 0.17$ ). Also, copolymers of higher HEMA content are more crosslinked due to the presence of diester in the HEMA monomer as explained earlier.

### Dynamic Swelling

Figures 4-6 present the dynamic swelling curves for the three systems. These plots show the general trend of increased swelling for the more hydrophilic materials in the series and faster attainment of the equilibrium values. The increasing rate of swelling suggests that not all curves can be fitted to an equation with the same functional dependence on  $t$ .

To elucidate the transport mechanism, the swelling curves were fitted for values up to  $M_t/M_\infty = 0.8$  to

$$M_t/M_\infty = kt^n \quad (1)$$

where  $M_t/M_\infty$  is the fractional water uptake by the polymer,  $t$  is diffusion time,  $k$  is a constant characteristic of the system, and  $n$  is an exponent characteristic of the mode of transport of the penetrant. This equation has been proposed as

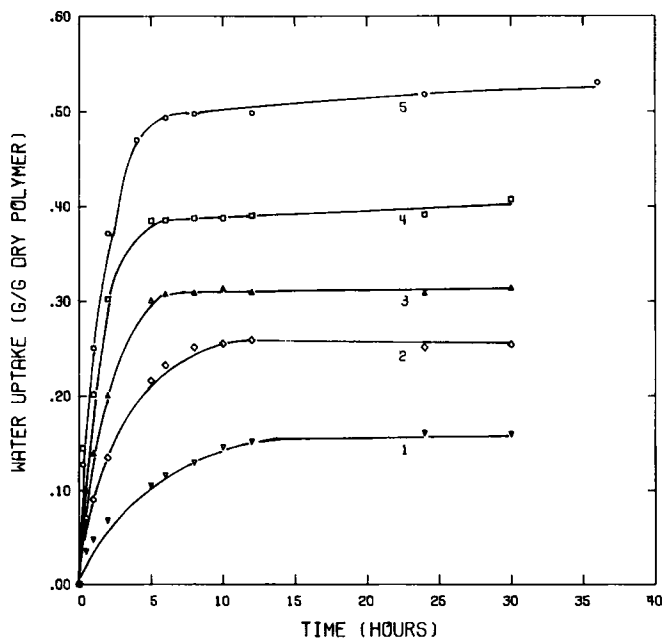


Fig. 4. Water uptake of P(HEMA-co-MMA) samples as a function of time at 37°C. Mole fraction of HEMA in copolymers: (1) 0.50; (2) 0.70; (3) 0.80; (4) 0.90; (5) 1.00.

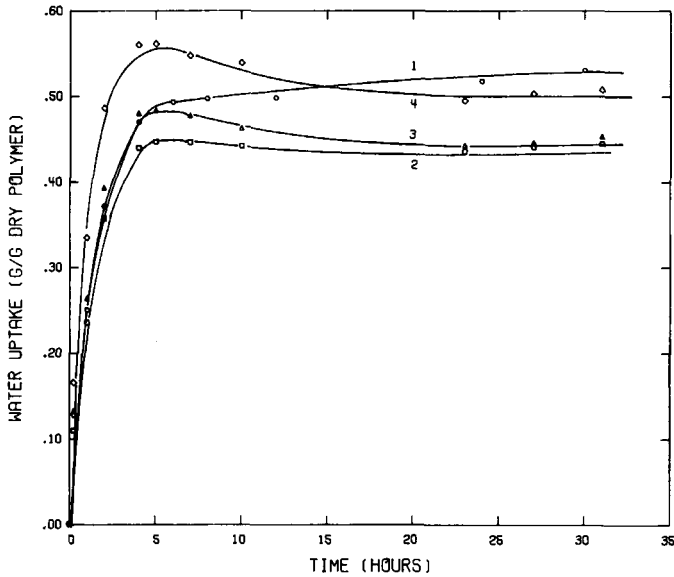


Fig. 5. Water uptake of P(HEMA-co-NVP) samples as a function of time at 37°C. Mole fractions of NVP in copolymers: (1) 0.00; (2) 0.10; (3) 0.20; (4) 0.30.

a simple method to analyze non-Fickian transport.<sup>20</sup> A value of  $n = 0.5$  indicates a Fickian mechanism, while  $n = 1$  indicates Case-II transport.<sup>8,9</sup>

Statistical analysis was performed on the values of  $n$  obtained from the linear regression, and the upper and lower 95% confidence intervals were determined (see the Appendix); these values are shown in Table III. Values of  $n$  ranged from

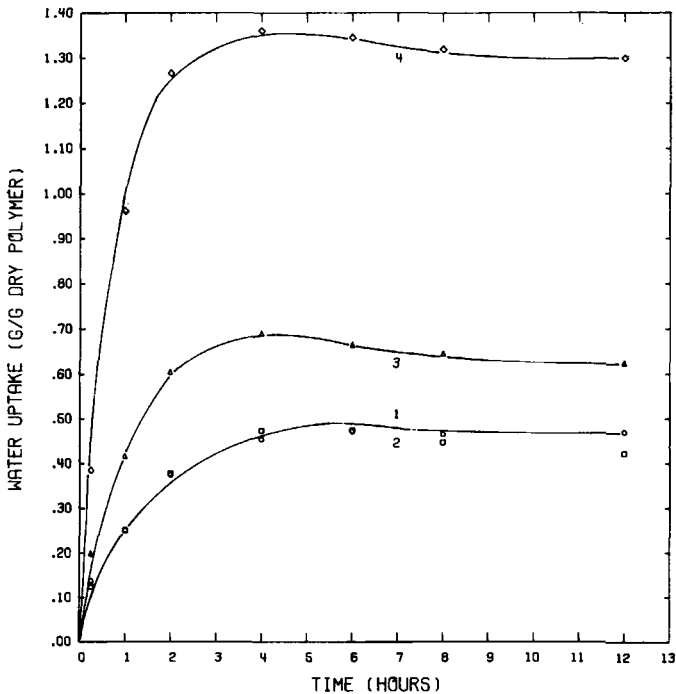


Fig. 6. Water uptake of P(HEMA-co-NVP) samples crosslinked with EGDMA as a function of time at 37°C. Mole fractions of NVP in copolymers: (1) 0.00; (2) 0.20; (3) 0.40; (4) 0.60.



TABLE III  
Analysis of Dynamic Swelling Experiments

Mole fraction HEMA	Mole fraction MMA	Mole fraction NVP	Wt % EGDMA	Kinetic exponent $n$	Lower limit of 95% confidence interval	Upper limit of 95% confidence interval	$r$	Number of samples
0.50	0.50	—	—	0.50	0.47	0.54	0.9982	3
0.70	0.30	—	—	0.50	0.32	0.68	0.9985	3
0.80	0.20	—	—	0.50	0.42	0.58	0.9999	3
0.90	0.10	—	—	0.52	0.24	0.79	0.9991	3
1.00	—	—	0.8	0.44	0.33	0.56	0.9941	2
1.00	—	—	—	0.48	0.37	0.59	0.9961	6
1.00	—	—	—	0.48	0.37	0.59	0.9961	6
0.90	—	0.10	—	0.53	0.40	0.67	0.9998	2
0.80	—	0.20	—	0.52	0.31	0.73	0.9995	2
0.70	—	0.30	—	0.52	0.47	0.57	1.0000	3
1.00	—	—	0.8	0.44	0.33	0.56	0.9941	2
0.80	—	0.20	0.8	0.53	0.29	0.78	0.9994	1
0.60	—	0.40	0.8	0.54	0.52	0.55	1.0000	1
0.40	—	0.60	0.8	0.59	0.23	1.42	0.9938	1

TABLE IV  
Analysis of Reswollen P(HEMA-co-MMA) Samples

Mole fraction HEMA	Mole fraction MMA	First swelling		Second swelling		Third swelling	
		$q_m$	$n$	$q_m$	$n$	$q_m$	$n$
0.50	0.50	0.1477	0.50	0.1635	0.50	0.1586	0.50
0.70	0.30	0.2436	0.50	0.2763	0.49	0.2753	0.50
0.80	0.20	0.3212	0.50	0.3724	0.49	0.3686	0.50
0.90	0.10	0.4110	0.52	0.4791	0.49	0.4951	0.50
1.00	—	0.6167	0.48	0.6339	0.50	0.6481	0.50

0.44 to 0.58 which indicate that the diffusion may be Fickian or anomalous depending on the copolymer composition, but not Case-II.

In judging the validity of these studies and the conclusion drawn, the upper and lower limit of the 95% confidence interval must also be examined. Indeed, values of the exponent  $n$  as high as 0.79 were determined.

Some of the dynamic swelling curves, especially those of P(HEMA-co-NVP) samples, exhibited a maximum value of  $q$ , which then decreased to the final, lower equilibrium value. This behavior may be due to unreacted monomer [for P(HEMA-co-NVP) systems] or uncrosslinked polymer chains diffusing out of the swollen polymer network. To verify this, the swollen materials were dried and the weight loss of the dry polymer determined. The polymer was reswollen to determine any change in  $q_m$  or  $n$ . Table IV presents the results of these studies.

A typical set of curves for the reswelling of a single composition is shown in Figure 7. Upon reswelling, the polymers had higher values of  $q_m$ , while the values

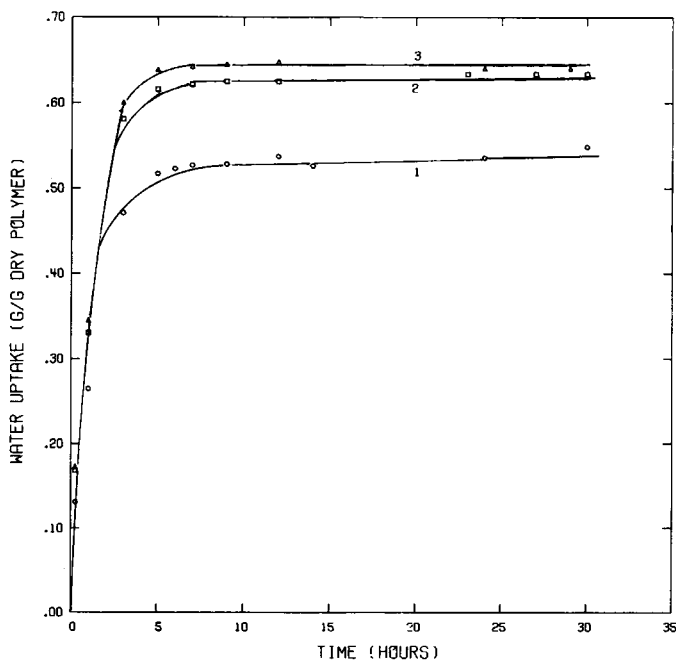


Fig. 7. Water uptake of a pure PHEMA sample as a function of time at 37°C: (1) first swelling; (2) second swelling; (3) third swelling.

of  $n$  remained essentially constant. The increase in  $q_m$  was larger for the more hydrophilic materials due to water expanding the polymer matrix which allows for more water to be imbibed by the polymer in subsequent swellings. The results of P(HEMA-co-MMA) given in Table IV indicate that the increases become smaller with repeated reswelling and will quickly reach a final value. No weight loss was observed after the first swelling.

## CONCLUSIONS

The transport of water through glassy copolymers of HEMA may be Fickian or non-Fickian, depending on the composition of the copolymers. Penetrant front movement indicates that non-Fickian transport predominates. However, the dynamic water swelling data analyzed by the exponential transport expression are not as conclusive, probably due to the small number of experimental points obtained, as judged by the associated statistical analysis.

## APPENDIX: STATISTICAL ANALYSIS OF EXPONENTIAL TRANSPORT EQUATION

The water transport data were fitted to eq. (A1), which can describe the general (not only Fickian) transport behavior of penetrants in polymers:

$$M_t/M_\infty = kt^n \quad (\text{A1})$$

Calculation of the exponent  $n$  was achieved by plotting the data in log-log plots according to eq. (A2) and using a linear regression to determine the slope:

$$\log(M_t/M_\infty) = \log k + n \log t \quad (\text{A2})$$

A simple point estimate of  $n$  can be misleading since the uncertainty associated with the calculated  $n$  value is not known. As a result, it is dangerous to base a conclusion on a specific value of  $n$  unless it can be shown that this value is known with precision. In this study a more meaningful estimate of  $n$  was obtained by calculating 95% confidence intervals for all reported values.

The "goodness of fit" of the regression model was measured by the sample correlation coefficient. This parameter is related to the percentage of total variation in the dependent variable that is explained by the regression model. The coefficient can take values from  $-1$  to  $+1$ . If the coefficient is near  $\pm 1$ , nearly 100% of the variation in the dependent variable is explained by the regression model; so the fit explains the relationship between the dependent and independent variables quite well.

## References

1. H. B. Hopfenberg, in *Membrane Science and Technology*, J. E. Flinn, Ed., Plenum, New York, 1970, p. 16.
2. T. Alfrey, Jr., E. F. Gurnee, and W. G. Lloyd, *J. Polym. Sci.*, **C12**, 249 (1961).
3. A. Peterlin, *Makromol. Chem.*, **124**, 136 (1969).
4. A. Peterlin, *Polym. Eng. Sci.*, **20**, 238 (1980).
5. T. T. Wang, T. K. Kwei, and H. L. Frisch, *J. Polym. Sci.*, **12**(7), 2019 (1969).
6. T. K. Kwei, T. T. Wang, and H. M. Zupko, *Macromolecules*, **5**, 645 (1972).
7. T. T. Wang and T. K. Kwei, *Macromolecules*, **6**, 919 (1973).
8. J. S. Vrentas, C. M. Jarzebski, and J. L. Duda, *AIChE J.*, **21**, 894 (1975).
9. J. S. Vrentas, C. M. Jarzebski, and J. L. Duda, *J. Polym. Sci., Polym. Phys. Ed.*, **15**, 441 (1977).
10. G. Astarita and G. C. Sarti, *Polym. Eng. Sci.*, **18**, 388 (1978).
11. G. C. Sarti, *Polymer*, **20**, 827 (1979).
12. N. L. Thomas and A. H. Windle, *Polymer*, **21**, 613 (1980).
13. N. L. Thomas and A. H. Windle, *Polymer*, **23**, 529 (1980).
14. H. B. Hopfenberg, A. Apicella, and D. E. Saleeby, *J. Membr. Sci.*, **8**, 273 (1981).

15. A. Apicella and H. B. Hopfenberg, *J. Appl. Polym. Sci.*, **27**, 1139 (1982).
16. D. E. Gregonis, C. M. Chen and J. D. Andrade, in *Hydrogels for Medical and Related Applications*, J. D. Andrade, Ed., ACS Symposium Series, Vol. 31, American Chemical Society, Washington, D.C., 1976, p. 88.
17. E. B. Nyquist, in *Functional Monomers*, R. H. Yocum and E. B. Nyquist, Eds., Marcel Dekker, New York, 1973, Vol. 1, p. 299.
18. P. S. Theocaris, *Moiré Fringes in Strain Analysis*, Pergamon, Oxford, 1969.
19. G. Astarita and S. Joshi, *J. Membr. Sci.*, **4**, 165 (1978).
20. H. L. Frisch, *Polym. Eng. Sci.*, **20**, 2 (1980).

Received September 1, 1982

Accepted October 29, 1982